Prognostic Value of ^{18}F-FDG PET/CT in a Large Cohort of Patients with Advanced Metastatic Neuroendocrine Neoplasms Treated with Peptide Receptor Radionuclide Therapy

Jingjing Zhang*[1], Qingxing Liu*[1,2], Aviral Singh[1,3], Christiane Schuchardt[1], Harshad R. Kulkarni[1], and Richard P. Baum[1]

[1]Theranostics Center for Molecular Radiotherapy and Precision Oncology, ENETS Center of Excellence, Zentralklinik Bad Berka, Bad Berka, Germany; [2]Department of Nuclear Medicine, Peking Union Medical College Hospital, Chinese Academy of Medical Sciences and Peking Union Medical College, Beijing, China; and [3]GROW–School for Oncology and Developmental Biology, Maastricht University, Maastricht, the Netherlands

The objective of this retrospective study was to determine the role of ^{18}F-FDG PET/CT in a large cohort of 495 patients with metastatic neuroendocrine neoplasms (NENs) who were treated with peptide receptor radionuclide therapy (PRRT) with a long-term follow-up. **Methods:** The 495 patients were treated with ^{177}Lu- or ^{90}Y-DOTATOC/DOTATATE PRRT between February 2002 and July 2018. All subjects received both ^{68}Ga-DOTATOC/TATE/NOC and ^{18}F-FDG PET/CT before treatment and were followed 3–189 mo. Kaplan–Meier analysis, log-rank testing (Mantel–Cox), and Cox regression analysis were performed for overall survival (OS) and progression-free survival (PFS). **Results:** One hundred ninety-nine patients (40.2%) presented with pancreatic NENs, 49 with cancer of unknown primary, and 139 with midgut NENs, whereas the primary tumor was present in the rectum in 20, in the lung in 38, in the stomach in 8, and in other locations in 42. ^{18}F-FDG PET/CT was positive in 382 (77.2%) patients and negative in 113 (22.8%) before PRRT, whereas 100% were ^{68}Ga-DOTATOC/TATE/NOC–positive. For all patients, the median PFS and OS, defined from the start of PRRT, were 19.6 mo and 58.7 mo, respectively. Positive ^{18}F-FDG results predicted shorter PFS (18.5 mo vs. 24.1 mo; $P = 0.0015$) and OS (53.2 mo vs. 83.1 mo; $P < 0.001$) than negative ^{18}F-FDG results. Among the cases of pancreatic NENs, the median OS was 52.8 mo in ^{18}F-FDG–positive subjects and 114.3 mo in ^{18}F-FDG–negative subjects ($P = 0.0006$). For all patients positive for ^{18}F-FDG uptake, and a ratio of more than 2 for the highest SUV_{max} on ^{68}Ga-somatostatin receptor (SSTR) PET to the most ^{18}F-FDG–avid tumor lesions, the median OS was 53.0 mo, compared with 43.4 mo in those patients with a ratio of less than 2 ($P = 0.030$). For patients with no ^{18}F-FDG uptake (complete mismatch imaging pattern), the median OS was 108.3 mo versus 76.9 mo for an SUV_{max} of more than 15.0 and an SUV_{max} of 15.0 or less on ^{68}Ga-SSTR PET/CT, respectively. **Conclusion:** The presence of positive lesions on ^{18}F-FDG PET is an independent prognostic factor in patients with NENs treated with PRRT. Metabolic imaging with ^{18}F-FDG PET/CT complements the molecular imaging aspect of ^{68}Ga-SSTR PET/CT for the prognosis of survival after PRRT. High SSTR expression combined with negative ^{18}F-FDG PET/CT results is associated with the most favorable long-term prognosis.

Key Words: peptide receptor radionuclide therapy; ^{18}F-FDG; neuroendocrine neoplasms; ^{177}Lu; ^{90}Y; prognostic factor

J Nucl Med 2020; 61:1560–1569
DOI: 10.2967/jnumed.119.241414

Neuroendocrine neoplasms (NENs) are a heterogeneous group of neoplasms and typically have a wide range of cellular differentiation with variable biologic aggressiveness and clinical outcome (*1*). The clinical course of NENs can be quite heterogeneous, with a variable response to the same treatment despite similar tumor characteristics. In principle, the choice of therapy depends on individual tumor characteristics and ranges from complete eradication to a watch-and-wait approach (*2–4*). NENs, especially those of the pancreas and intestine, are frequently identified at a late stage at which there is advanced metastatic disease.

Most well-differentiated NENs are characterized by a high level of expression of the somatostatin receptors (SSTRs), allowing the use of radiolabeled somatostatin analogs for SSTR-targeted imaging (i.e., ^{111}In-octreotide scintigraphy or ^{68}Ga-SSTR PET) as well as peptide receptor radionuclide therapy (PRRT) using ^{177}Lu- or ^{90}Y-labeled somatostatin analogs (DOTATATE or DOTATOC). PRRT has been established as an efficient and well-tolerated treatment for patients with unresectable or metastatic progressive well-differentiated SSTR-positive neuroendocrine tumors (*5*) and is shown to be highly efficacious in terms of progression-free survival (PFS) and response rates compared with other treatment modalities (*6–8*). Quality of life is also significantly improved after PRRT (*7,9,10*). The significant benefit of PRRT over cold somatostatin analog therapy demonstrated by the landmark randomized phase III clinical trial (NETTER-1) (*7*) led to the approval of ^{177}Lu-DOTATATE (Lutathera; Advanced Accelerator Applications) by both the European Medicines Agency and the U.S. Food and Drug Administration for the treatment of gastroenteropancreatic neuroendocrine tumors.

Received Dec. 24, 2019; revision accepted Mar. 5, 2020.
For correspondence or reprints contact: Jingjing Zhang, Theranostics Center for Molecular Radiotherapy and Precision Oncology, Zentralklinik Bad Berka, Robert-Koch-Allee 9, 99437 Bad Berka, Germany.
E-mail: zhangjingjingtag@163.com
*Contributed equally to this work.
Published online Mar. 13, 2020.

With the growing importance of PRRT in treating NENs, the relevant outcome predictors are becoming increasingly significant to optimize the application of PRRT. Several prognostic factors of NENs after PRRT have been described, including gene cluster expression (*11*), site of the primary tumor (*12,13*), presence of metastases (*13*), resection of the primary tumor (*14*), grade of differentiation (*13,15–17*), proliferation index (Ki-67 index) (*13,18–20*), serum biomarkers (*18,21*), presence of SSTRs (*22,23*), tumor stage (*24*), and treatment modality (*18,25,26*). However, several of these factors are difficult to assess, especially in the setting of multifocal metastatic disease. One such example is the most commonly used proliferation index, Ki-67. The histopathology of a certain small part of the tumor from biopsy or resected specimens may not be representative of the entire tumor burden; therefore, whole-body noninvasive alternatives may offer significant advantages (*27*).

SSTR imaging (PET or scintigraphy) represents an estimation of the SSTR status for planning of PRRT and for evaluation of response to the treatment. ^{18}F-FDG PET/CT is used to assess glycolytic metabolism, characterized by the potential for malignancy. SSTR imaging seems like a promising alternative to repeated tissue sampling for the determination of the aggressiveness of tumors, since the results have been found to be associated with tumor aggressiveness and are highly prognostic in a variety of tumors (*28–31*). The diagnostic value of ^{18}F-FDG PET in lower-grade (1, II, and IIIa) NENs is limited since they represent the slowly proliferating tumors with lower glycolytic activity. ^{18}F-FDG PET/CT or PET/MRI is not used for diagnosis of NENs and currently is not a routine diagnostic for NENs before PRRT.

The aim of our study was to evaluate the role of baseline ^{18}F-FDG PET/CT in predicting the PFS and overall survival (OS) of a large cohort of patients with metastatic NENs treated with PRRT with a long-term follow-up.

TABLE 1
Demographics of Patients with NENs (n = 495)

Demographic	Data
Sex	
Male	299 (60.4)
Female	196 (39.6)
Age (y)	
Median	59.0 ± 10.7
y ≤50	111 (22.4)
50< y ≤60	146 (29.5)
60< y ≤70	165 (33.3)
70< y ≤80	73 (14.7)
Primary tumor site	
Cancer of unknown primary	49 (9.9)
Lung	38 (7.7)
Midgut	139 (28.1)
Others	42 (8.5)
Pancreas	199 (40.2)
Rectum	20 (4.0)
Stomach	8 (1.6)
Ki-67 index grading	
G1 (Ki-67 < 3%)	117 (23.6)
G2 (Ki-67 = 3%–20%)	245 (49.5)
G3 (Ki-67 > 20%)	29 (5.9)
Not assessed	104 (21.0)

Qualitative data are numbers followed by percentages in parentheses; continuous data are medians.

MATERIALS AND METHODS

Patients

From February 2002 to July 2018, a retrospective data analysis was performed for a total of 495 patients with advanced NENs who received PRRT at Zentralklinik Bad Berka and underwent PET/CT imaging with both ^{68}Ga-SSTR and ^{18}F-FDG at baseline before therapy. Patients with histopathologically confirmed metastatic NENs and a high level of SSTR expression, that is, tumor uptake greater than or equal to normal liver parenchyma uptake on ^{68}Ga-SSTR PET imaging, were included. Disease progression was documented within 3–6 mo before the start of PRRT. The study was approved by the institutional review board, and written informed consent was obtained from each patient. The baseline demographics of the patients are shown in Table 1.

PRRT Regimen

The DOTA-conjugated somatostatin analogs DOTATOC, DOTANOC, and DOTATATE were labeled with ^{68}Ga for SSTR PET imaging and either ^{177}Lu or ^{90}Y for PRRT, in accordance with good-manufacturing-practice regulations. PRRT regimens conformed with the published practical guidelines for PRRT (*32*). The labeling of DOTA-conjugated peptides with ^{177}Lu and ^{90}Y was performed according to a previously published method (*16,33*). High-performance liquid chromatography was used for quality control. Radiochemical purity was always higher than 98%. An in-house–produced amino acid infusion (1,600 mL of 5% lysine HCl and 10% L-arginine HCl) was administered for nephroprotection during each PRRT cycle (*34*). Additional nephroprotection using an intravenous infusion of 4% Gelofusine (B. Braun Melsungen AG) adjusted to patients' weight (infusion as a bolus of 1 mL/kg of body weight over 10 min before therapy and followed by 0.02 mL/kg/min over 3 h after radiopeptide infusion) was applied in cases of impaired renal function (glomerular filtration rate < 60 mL/min) and in patients treated with ^{90}Y (*16,32*). The infusion was started at least 30 min before administration of the radiopharmaceutical and lasted for 4 h afterward. The radiopharmaceutical was coadministered over 10–15 min using a second infusion pump system. The administrated radioactivity was individually calculated on the basis of the Bad Berka Score (*8,16,34*).

Response Assessment

The treatment response was evaluated on CT or MRI according to RECIST 1.1 (*35*) and by PET imaging according to the criteria of the European Organization for Research and Treatment of Cancer (*36,37*). Imaging was performed before each PRRT cycle and at restaging. Restaging was performed every 3–4 mo after PRRT, and every 6 mo for stable disease or remission (complete or partial) after initial follow-up, until disease progression. PRRT was resumed if progression occurred after a therapy interval of more than 6 mo (the so-called next treatment phase of PRRT) (*10,16*). A decision on whether to use a salvage approach considering PRRT after

TABLE 2
Baseline ^{68}Ga-SSTR and ^{18}F-FDG PET Imaging of Patients with NENs

Parameter	Data
^{68}Ga-SSTR uptake	495 (100.0)
SUV_{max} = liver (level 1)	3 (0.6)
Liver<SUV_{max}≤15 (level 2)	161 (32.5)
15<SUV_{max}≤20 (level 3)	106 (21.4)
SUV_{max}>20 (level 4)	225 (45.5)
^{18}F-FDG uptake	495 (100.0)
Positive	382 (77.2)
Negative	113 (22.8)
Primary tumor uptake on ^{18}F-FDG PET	
No uptake (level 1)	376 (76.0)
SUV_{max}≤10 (level 2)	87 (17.6)
10<SUV_{max}≤15 (level 3)	16 (3.2)
SUV_{max}>15 (level 4)	16 (3.20)
Primary tumor uptake on ^{68}Ga-SSTR	
No uptake (level 1)	262 (52.9)
SUV_{max}≤15 (level 2)	102 (20.6)
15<SUV_{max}≤20 (level 3)	37 (7.5)
SUV_{max}>20 (level 4)	94 (19.0)
Liver tumor burden on ^{18}F-FDG PET	
0 lesions (level 1)	239 (48.3)
1 lesion (level 2)	49 (9.9)
2 to ≤5 lesions (level 3)	126 (25.5)
>5 lesions (level 4)	77 (15.6)
Not assessed	4 (0.8)
Bone tumor burden on ^{18}F-FDG PET	
0 lesions (level 1)	409 (82.6)
1 lesion (level 2)	29 (5.9)
2 to ≤5 lesions (level 3)	36 (7.3)
>5 lesions (level 4)	19 (3.8)
Not assessed	2 (0.4)
Lymph node tumor burden on ^{18}F-FDG PET	
0 lesions (level 1)	362 (73.1)
1 lesion (level 2)	55 (11.1)
2 to ≤5 lesions (level 3)	58 (11.7)
>5 lesions (level 4)	13 (2.6)
Not assessed	7 (1.4)
Lung tumor burden on ^{18}F-FDG PET	
0 lesions (level 1)	463 (93.5)
1 lesion (level 2)	22 (4.4)
2 to ≤5 lesions (level 3)	6 (1.2)
>5 lesions (level 4)	4 (0.8)
Liver tumor burden on ^{68}Ga-SSTR PET	
0 lesions (level 1)	76 (15.4)
1 lesion (level 2)	32 (6.5)
2 to ≤5 lesions (level 3)	153 (30.9)
>5 lesions (level 4)	234 (47.3)
Liver tumor ^{68}Ga-SSTR uptake	
No uptake (level 1)	77 (15.6)
SUV_{max}≤15 (level 2)	117 (23.6)
15<SUV_{max}≤20 (level 3)	90 (18.2)
SUV_{max}>20 (level 4)	211 (42.6)

Data are numbers followed by percentages in parentheses.

progression was made by internal or external tumor boards. SSTR PET/CT and ^{18}F-FDG PET/CT (until January 2014 with Biograph and since then with Biograph mCT Flow 64; Siemens Medical Solutions) was performed in all cases 45–90 min after the intravenous injection of 46–260 MBq of ^{68}Ga-DOTANOC, ^{68}Ga-DOTATOC, or ^{68}Ga-DOTATATE and 45–90 min after the intravenous injection of 350–600 MBq of ^{18}F-FDG, respectively. PET/CT images were acquired from the skull to the middle part of the thigh. Contrast-enhanced CT (spiral CT using a Biograph mCT Flow 64) was acquired after the intravenous administration of 60–100 mL of nonionic iodinated contrast agent. SUV_{max} was obtained by drawing circular regions of interest (ROIs), which were automatically adapted (40% isocontour) to a 3-dimensional volume of interest using commercial software provided by the vendor. Images were evaluated by 2 experienced nuclear medicine specialists. MRI was performed in selected cases (allergy to iodinated contrast agent or poor detectability of liver metastases on CT), and routine sonography was performed for additional diagnostic evaluation.

Data Analysis

Data were collected in the following categories: patient characteristics, tumor characteristics, prior treatments, baseline ^{68}Ga-SSTR PET/CT results, baseline ^{18}F-FDG PET/CT results, PRRT radionuclide, PRRT cycle, cumulative activity, all completed ^{68}Ga-SSTR and ^{18}F-FDG PET/CT results, and follow-up. Progression was determined on the basis of RECIST or the criteria of the European Organization for Research and Treatment of Cancer. The categories of tumor uptake and tumor burden on ^{68}Ga-SSTR and ^{18}F-FDG PET/CT are listed in Table 2.

Statistical Analysis

The primary and secondary endpoints of this study were the duration of OS and PFS, respectively, defined from the start of PRRT. Survival curves for PFS and OS were estimated by Kaplan–Meier analysis, and significance was tested by the log-rank test. Univariate analysis was conducted for each prognostic factor using the log-rank test. Multivariate analysis (Cox proportional-hazards model) was performed to estimate hazard ratios (HRs) and 95% confidence intervals (95% CIs) for the potential prognostic factors. Quantitative data were denoted as mean ± SD. The statistical analysis was 2-tailed and conducted by SPSS software (IBM). A P value of less than 0.05 was considered statistically significant.

RESULTS

Patient Characteristics

The characteristics of the 495 patients (299 men, 196 women; median age at first treatment, 59.0 ± 10.7 y; range, 19–80 y) are shown in Tables 1 and 2. Primary tumors were localized in the pancreas in 199 (40.2%) patients, midgut in 139 (28.1%), lung in 38 (7.7%), rectum in 20 (4.0%), stomach in 8 (1.6%), and other locations in 42 (8.5%); 49 (9.9%) patients had cancer of unknown primary. Most patients (117 and 245, respectively) had well-differentiated NENs of grade 1 (23.6%) or grade 2 (49.5%). At baseline, 382 patients (77.2%) were ^{18}F-FDG–positive, and 113 (22.8%) were ^{18}F-FDG–negative. The number of treatment cycles and the cumulative administered radioactivity are listed in Supplemental Table 1 (supplemental materials are available at http://jnm.snmjournals.org). Four hundred fifteen (83.8%) patients received dual PRRT, that is, a combination of ^{177}Lu and ^{90}Y; 60 (12.1%) received ^{177}Lu as monotherapy, and 20 (4.0%) received ^{90}Y as monotherapy. The mean cumulative administered

radioactivity for all patients was 25.7 ± 10.8 GBq (range, 3.9–60.7 GBq).

Univariate and Multivariate Analysis for OS and PFS

The results of univariate and multivariate analysis of possible prognostic factors for OS and PFS are listed in Tables 3–6. Over a median follow-up of 94 mo for all patients (range, 3–189 mo), 319 patients (64.4%) died and 136 patients (27.5%) progressed. The median OS and PFS of the entire cohort were 58.7 mo (95% CI, 52.8–64.6) and 19.6 mo (95% CI, 17.6–21.7), respectively (Fig. 1).

Tumor grading was an independent predictor for both OS ($P = 0.012$) and PFS ($P = 0.039$). A higher tumor grade was associated with worse prognosis. The median OS in grades 1, 2, and 3 was 78.5 mo (95% CI, 66.2–90.8), 55.4 mo (95% CI, 46.9–63.9), and 33.2 mo (95% CI, 18.8–47.6), respectively. When compared with grade 1, grade 2 had a 1.4-fold increase in the risk of death (95% CI, 1.0–2.0; P, 0.038), whereas grade 3 was associated with a 2.5-fold increase (95% CI, 1.3–4.5; $P = 0.004$). The median PFS in grades 1, 2, and 3 was 23.0 mo (95% CI, 15.9–30.2), 18.9 mo (95% CI, 15.2–22.6), and 7.5 mo (95% CI, 0.0–20.1), respectively. When compared with grade 1, grade 2 tumors had a 1.2-fold increase in the risk of progression (95% CI, 0.9–1.5; $P = 0.150$), whereas G3 was associated with a 2.1-fold increased risk of progression (95% CI, 1.3–3.4; $P = 0.003$).

Primary tumor site was an independent predictor of OS ($P = 0.004$). The median OS of patients with pancreas, midgut, and lung NENs was 54.4 mo (95% CI, 49.3–59.6), 77.8 mo (95% CI, 61.0–94.6), and 46.2 mo (95% CI, 34.1–58.3), respectively. The median PFS was 25.8 mo (95% CI, 21.8–29.8), 22.6 mo (95% CI, 17.2–28.0), and 10.6 mo (95% CI, 5.0–16.1), respectively.

^{18}F-FDG Uptake Status Related to Survival

In all patients, median OS and PFS were significantly higher in the ^{18}F-FDG–negative group than in the ^{18}F-FDG–positive group. The benefit in OS was 83.1 mo (95% CI, 57.0–109.2) versus 53.2 mo (95% CI, 49.4–57.0; $P < 0.001$), respectively, and in PFS, 24.1 (95% CI, 19.9–28.3) versus 18.5 mo (95% CI, 15.9–21.1; $P < 0.002$), respectively (Fig. 2). ^{18}F-FDG–negative status was an independent prognostic factor for OS, with a 0.5-fold decrease in the risk of death (HR, 0.5; 95% CI, 0.3–0.8; $P = 0.002$), as well as for PFS, with a 0.7-fold decrease in the risk of progression (HR, 0.7; 95% CI, 0.5–0.9; $P = 0.007$). ^{18}F-FDG–positive lymph node and liver tumor burden was an

TABLE 3
Univariate and Multivariate Analyses of Potential Factors Contributing to OS, Part 1

Factors	OS (mo)		Univariate analysis (*P*)	Multivariate analysis	
	Median	95% CI		HR and 95% CI	*P*
All patients	58.7	52.8–64.6			
Sex					
Male	53.7	47.6–59.8	0.040		
Female	66.1	54.4–77.8			
Age (y)					
y ≤50	69.8	61.7–77.8	0.024		
50< y ≤60	61.6	51.5–71.7			
60< y ≤70	53.0	49.8–56.3			
70< y ≤80	49.0	39.6–58.5			
Grading					
Grade 1	78.5	66.2–90.8	<0.001		0.012
Grade 2	55.4	46.9–63.9		1.4 (1.0–2.0)	0.038
Grade 3	33.2	18.8–7.6		2.5 (1.3–4.5)	0.004
Not assessed	54.1	48.3–59.9		1.6 (1.1–2.2)	0.009
^{18}F-FDG PET uptake					
Positive	53.2	49.4–57.0	<0.001		0.002
Negative	83.1	57.0–109.2		0.5 (0.3–0.8)	
Primary tumor site					
Cancer of unknown primary	65.1	47.4–82.7	0.007		0.004
Lung	46.2	34.1–58.3		0.3 (0.1–0.7)	0.004
Midgut	77.8	61.0–94.6		0.7 (0.3–1.6)	0.344
Others	65.7	31.3–100.1		0.3 (0.1–0.7)	0.008
Pancreas	54.4	49.3–59.6		0.4 (0.2–1.0)	0.041
Rectum	55.4	50.3–60.4		0.5 (0.2–1.0)	0.063
Stomach	46.9	33.3–60.5		0.6 (0.2–1.5)	0.239

TABLE 4
Univariate and Multivariate Analyses of Potential Factors Contributing to OS, Part 2

Factors	OS (mo)		Univariate analysis (*P*)	Multivariate analysis	
	Median	95% CI		HR and 95% CI	*P*
Liver tumor burden on ^{18}F-FDG PET					
0 lesions	75.6	65.5–85.6	<0.001		0.034
1 lesion	55.4	36.9–73.9		1.7 (0.6–5.2)	0.338
2 to ≤5 lesions	47.1	40.5–53.7		1.2 (0.4–3.8)	0.712
>5 lesions	43.7	35.4–52.0		2.2 (0.7–6.4)	0.157
Not assessed	54.6	33.7–75.5		2.3 (0.8–7.0)	0.127
Bone tumor burden on ^{18}F-FDG PET					
0 lesions	61.6	54.9–68.3	0.004		
1 lesion	56.0	29.6–82.4			
2 to ≤5 lesions	41.9	25.1–58.8			
>5 lesions	43.4	19.2–67.7			
Not assessed	32.6	—			
Lymph node tumor burden on ^{18}F-FDG PET					
0 lesions	63.8	56.3–71.4	0.006		0.035
1 lesion	51.6	34.6–68. 5		1.4 (0.5–4.1)	0.540
2 to ≤5 lesions	46.2	37.2–55.3		1.7 (0.6–5.2)	0.344
>5 lesions	37.4	10.0–64.7		1.8 (0.6–5.4)	0.293
Not assessed	86.6	23.7–149.6		4.4 (1.3–15.3)	0.018
Grading of PRRT					
2 to ≤3 cycles	33.27	25.0–41.3	<0.001		<0.001
4 to ≤5 cycles	51.6	44.5–58.7		7.9 (3.9–15.9)	<0.001
6 to ≤7 cycles	68.9	61.8–76.1		4.7 (2.6–8.4)	<0.001
8 to ≤10 cycles	122.5	84.8–160.3		3.0 (1.8–5.0)	<0.001
Cumulative activity (GBq)					
Activity ≤15	26.0	13.8–38.2	<0.001		0.038
15< activity ≤25	52.7	45.4–59.9		1.1 (0.6–2.0)	0.745
25< activity ≤35	61.1	54.9–67.3		0.7 (0.4–1.1)	0.084
Activity >35	77.8	66.0–89.6		0.8 (0.6–1.2)	0.379

independent predictor for OS ($P = 0.035$ and $P = 0.034$, respectively), whereas ^{18}F-FDG–avid bone tumor burden (metastases) was an independent predictor for PFS ($P = 0.001$).

In the ^{177}Lu-PRRT subgroup, median OS and PFS were significantly higher in the ^{18}F-FDG–negative group than in the ^{18}F-FDG–positive group (median OS, 97.7 mo vs. 51.0 mo [$P < 0.01$]; median PFS, 33.8 mo vs. 19.9 mo [$P < 0.05$]) (Fig. 3).

In the pancreatic NEN subgroup, median OS and PFS were significantly higher in the ^{18}F-FDG–negative than in the ^{18}F-FDG–positive group (median OS, 114.3 mo vs. 52.8 mo; median PFS, 36.9 mo vs. 22.4 mo [$P < 0.001$ for both]) (Fig. 4).

In the midgut NEN subgroup, the median OS was 95.3 mo in the ^{18}F-FDG–negative group and 62.1 mo in the ^{18}F-FDG PET–positive group. The median PFS was 36.1 mo in the ^{18}F-FDG–negative group and 29.0 mo in the ^{18}F-FDG PET–positive group.

^{68}Ga-SSTR PET Imaging Related to Survival

^{68}Ga-SSTR uptake in the primary tumor was an independent predictor of OS ($P = 0.011$) and PFS ($P = 0.003$). In multivariate analysis, compared with level 1 liver tumor burden in ^{68}Ga-SSTR PET, level 2 had a significant decreased risk of progression, with an HR of 0.5 (95% CI, 0.3–0.7; $P = 0.001$), but levels 3 and 4 had no significant decrease in risk (level 3: HR, 0.9; 95% CI, 0.5–1.5 [$P = 0.664$]; level 4: HR, 0.9; 95% CI, 0.6–1.1 [$P = 0.256$]).

The statistical analysis revealed that the highest SUV_{max} of all target (SSTR-positive) lesions on ^{68}Ga-SSTR PET for each patient was not significant in terms of OS or PFS, and there was no direct correlation between OS and the highest SUV_{max} of all target tumor lesions ($P > 0.05$). The analysis of OS showed no significant difference between patients with an SUV_{max} of less than 15 and patients with an SUV_{max} of more than 15 on ^{68}Ga-SSTR PET imaging, including those from the midgut NEN subgroup and the ^{18}F-FDG–negative group. For ^{18}F-FDG–positive patients with a ratio of more than 2 for maximum SSTR to ^{18}F-FDG (the highest SUV_{max} among all target lesions on ^{68}Ga-SSTR PET to the most ^{18}F-FDG–avid tumor lesions for each patient), the median OS was 53.0 mo, compared with 43.4 mo for patients

TABLE 5
Univariate and Multivariate Analyses of Potential Factors Contributing to PFS, Part 1

Factors	PFS (mo)		Univariate analysis (*P*)	Multivariate analysis	
	Median	95% CI		HR and 95% CI	*P*
All patients	19.6	17.6–21.7			
Age					
y ≤50	25.0	19.4–30.5	0.281		
50< y ≤60	18.4	12.8–23.9			
60< y ≤70	17.9	15.1–20.7			
70< y ≤80	22.4	16.8–28.0			
Grading					
Grade 1	23.0	15.9–30.2	0.003		0.039
Grade 2	18.9	15.2–22.6		1.2 (0.9–1.5)	0.150
Grade 3	7.5	0.0–20.1		2.1 (1.3–3.4)	0.003
Not assessed	19.8	13.8–25.7		1.1 (0.9–1.5)	0.426
^{18}F-FDG PET uptake					
Positive	18.5	15.9–21.1	0.002		0.007
Negative	24.1	19.9–28.3		0.7 (0.5–0.9)	
Primary tumor site					
Cancer of unknown primary	11.4	6.5–16.2	0.011		
Lung	10.6	5.0–16.1			
Midgut	22.6	17.2–28.0			
Others	9.1	2.7–15.5			
Pancreas	25.8	21.8–29.8			
Rectum	19.9	11.8–27.9			
Stomach	24.6	18.9–30.4			

with a ratio of less than 2 ($P = 0.030$). For ^{18}F-FDG–negative patients, the median OS was 108.3 mo, versus 76.9 mo for an SUV_{max} of more than 15.0 and an SUV_{max} of 15.0 or less on ^{68}Ga-SSTR PET, respectively.

DISCUSSION

To the best of our knowledge, to date this study represents the largest cohort of metastatic NEN patients treated with personalized PRRT in which long-term prognosis was evaluated on the basis of initial dual PET tracer imaging (^{68}Ga-SSTR PET/CT and ^{18}F-FDG PET/CT). All patients were followed up until death (64.4% of the patients) or the study cutoff date (end of 2018). The follow-up (median, 94 mo; range, 3–189 mo) in this patient cohort is the longest among all published relevant studies (*16*).

SSTR PET/CT imaging with ^{68}Ga-labeled somatostatin analogs has excellent sensitivity and specificity for diagnosing and staging NENs (*38,39*). ^{18}F-FDG PET is widely used in oncology, but its use in neuroendocrine tumors has been a matter of controversy (*40*). Several studies have demonstrated the association of ^{18}F-FDG PET with treatment response and PFS after PRRT in NENs. In a study with 98 NEN patients, an ^{18}F-FDG SUV_{max} of more than 3 was found to be the only independent predictor of PFS, and an ^{18}F-FDG SUV_{max} of more than 9 was strongly correlated with a greater risk of mortality, although median OS was not reached (*27*). Sansovini et al. reported a phase II trial of ^{177}Lu-DOTATATE PRRT in 60 patients with locally advanced or metastatic well-differentiated grade 1 or 2 pancreatic neuroendocrine tumors who completed the scheduled 5 cycles of PRRT. The median PFS was 21.1 mo in ^{18}F-FDG–positive patients (58%) and 68.7 mo in the ^{18}F-FDG–negative group regardless of the total activity administered ($P < 0.0002$) (*41*), but the uptake on SSTR imaging, before and after therapy, was not significant in terms of PFS (*42*). Chan et al. reported a NETPET grading scheme for dual SSTR and ^{18}F-FDG PET/CT imaging in a study with 62 NEN patients. The NETPET grade divided subjects into solely SSTR-positive, SSTR-positive/^{18}F-FDG–positive, and SSTR-negative/^{18}F-FDG–positive subgroups and introduced a 0–5 categoric scale based largely on the characteristics of the single initial lesion, showing promise as a prognostic imaging biomarker in neuroendocrine tumors (*43*). Our group also has demonstrated that PET/CT imaging with ^{18}F-FDG along with SSTR helps to stratify patients with World Health Organization grade 3 NENs (*16*).

The median OS of the current study after PRRT was 58.7 mo, which is within the range reported in the literature (*18*). The median PFS was 19.6 mo, which was shorter than in other studies, as the treatment response was evaluated according to both RECIST and molecular imaging criteria. Moreover, the current study included 128 patients who received up to 3 cycles of PRRT only, which may have influenced the prognosis.

TABLE 6
Univariate and Multivariate Analyses of Potential Factors Contributing to PFS, Part 2

Factors	PFS (mo)			Multivariate analysis	
	Median	95% CI	Univariate analysis (*P*)	HR and 95% CI	*P*
Liver tumor burden on ^{18}F-FDG PET					
0 lesions	20.8	17.4–24.1	0.034		
1 lesion	27.8	20.9–34.7			
2 to ≤5 lesions	16.2	11.5–20.9			
>5 lesions	17.9	14.1–21.7			
Not assessed	28.2	0.0–58.7			
Bone tumor burden on ^{18}F-FDG PET					
0 lesions	22.4	19.3–25.5	<0.001		0.001
1 lesion	13.3	1.4–25.1		1.0 (0.2–4.1)	0.982
2 to ≤5 lesions	10.5	8.4–12.5		1.7 (0.4–7.4)	0.479
>5 lesions	11.5	0.0–24.9		2.2 (0.5–9.4)	0.304
Not assessed	12.0	—		1.2 (0.3–5.2)	0.848
Lymph node tumor burden on ^{18}F-FDG PET					
0 lesions	21.6	18.6–24.7	<0.001		0.050
1 lesion	17.9	10.9–25.0		1.2 (0.5–3.1)	0.587
2 to ≤5 lesions	15.4	12.3–18.6		1.3 (0.5–3.4)	0.552
>5 lesions	6.5	4.5–8.5		1.3 (0.5–3.3)	0.563
Not assessed	37.2	7.1–67.3		3.5 (1.2–10.1)	0.019
Lung tumor burden on ^{18}F-FDG PET					
0 lesions	19.9	17.5–22.3	<0.001		
1 lesion	18.4	16.5–20.3			
2 to ≤5 lesions	3.7	0.0–21.3			
>5 lesions	5.3	1.5–9.2			
Grading of PRRT					
2 to ≤3 cycles	13.6	8.6–18.5	0.907		
4 to ≤5 cycles	18.0	15.2–20.8			
6 to ≤7 cycles	25.0	20.9–29.2			
8 to ≤10 cycles	26.8	16.7–36.8			

Meanwhile, this study included not only grade 1 and 2 NENs but also high-risk grade 3 NENs, as well as patients with variable primary tumor sites. In this study, both tumor grade and primary tumor site were found to be independent predictors for OS. Patients with midgut NENs had the longest median OS, 77.8 mo; whereas, median OS was 55.4 mo in the rectal NEN group, 54.4 in the pancreatic NEN group, and 46.2 mo in the lung NEN group.

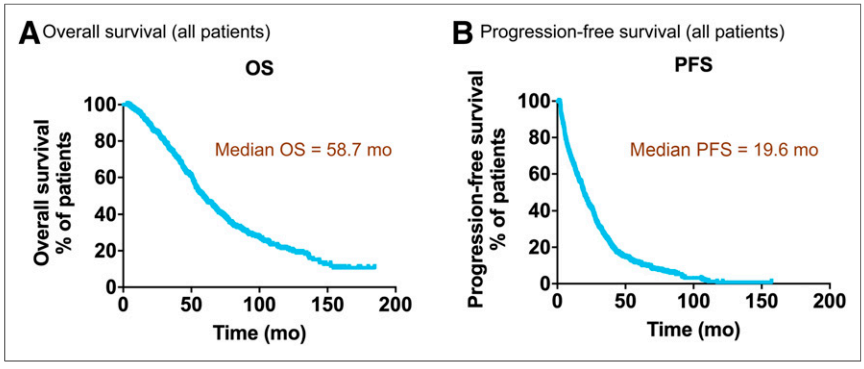

FIGURE 1. Kaplan–Meier curves of OS and PFS for all patients (n = 495). (A) Median OS was 58.7 mo (95% CI, 52.8–64.6). (B) Median PFS was 19.6 mo (95% CI, 17.6–21.7).

Our results demonstrated that an ^{18}F-FDG–negative tumor status was an independent prognostic factor for OS of PRRT, with a 0.5-fold decrease in the risk of death. Although not generally used for the diagnosis of NENs, ^{18}F-FDG PET/CT was able to classify NEN patients into different prognostic categories for PRRT. A very high SUV on ^{18}F-FDG PET would at least lead to reconsideration of the decision to perform PRRT as the first-line procedure. We would suggest that the decision to perform ^{18}F-FDG PET/CT be based on personalized medicine criteria, especially the grade, time course of the disease, speed of progression, total tumor mass, and other

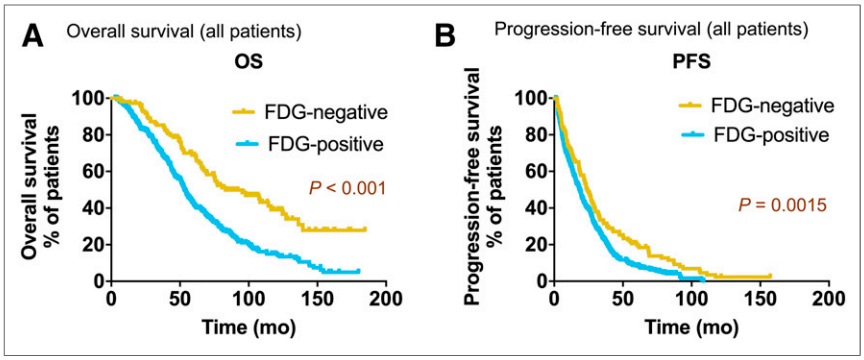

FIGURE 2. Kaplan–Meier survival analysis of all NEN patients ($n = 495$) stratified by baseline ^{18}F-FDG status. Patients with ^{18}F-FDG–negative lesions had significantly higher median OS (A) (83.1 mo vs. 53.2 mo, $P < 0.001$) and higher median PFS (B) (24.1 mo vs. 18.5 mo, $P < 0.002$) than patients with ^{18}F-FDG–positive lesions.

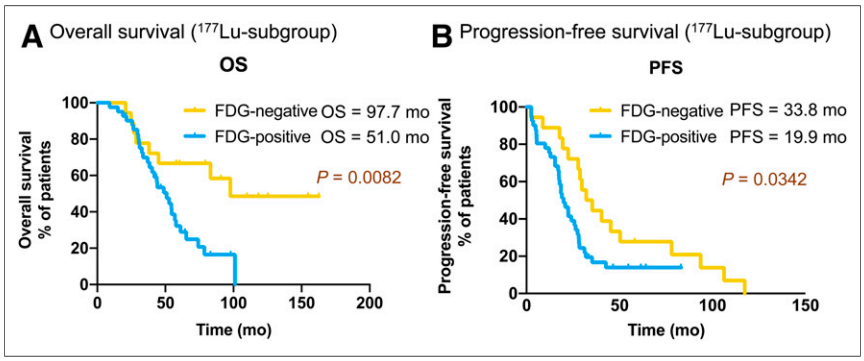

FIGURE 3. Kaplan–Meier curves of OS (A) and PFS (B) for ^{177}Lu subgroup ($n = 60$) stratified by baseline ^{18}F-FDG status.

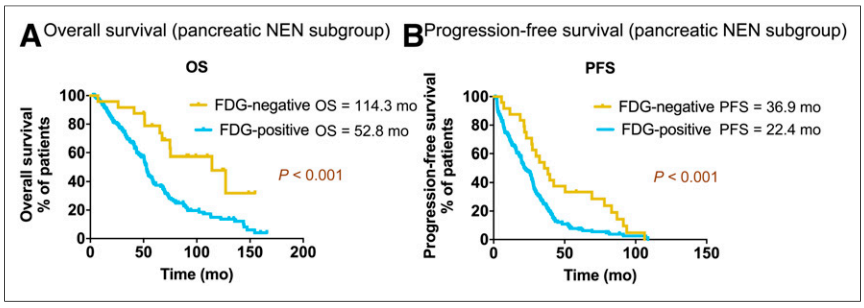

FIGURE 4. Kaplan–Meier survival of OS (A) and PFS (B) for pancreatic NEN subgroup ($n = 199$) stratified by baseline ^{18}F-FDG status.

criteria as previously published regarding the Bad Berka score (*8,16,34*).

SSTR imaging is a positive prognostic factor for demonstrating the abundance of SSTR expression, which is intensely related to well-differentiated tumor and therefore used for evaluating the possibility of treatment with cold and radiolabeled somatostatin analogs (*44*). In this study, ^{68}Ga-SSTR uptake in the primary tumor was an independent predictor of OS and PFS, as agrees with other studies. However, the prognostic value of ^{68}Ga-SSTR PET imaging was lower than that of ^{18}F-FDG PET. There was no direct correlation between the single highest SUV_{max} of ^{68}Ga-SSTR PET and OS. For all patients with ^{18}F-FDG uptake (NETPET SSTR-positive/^{18}F-FDG–positive disease) and a ratio of more than 2 for the highest SUV_{max} on ^{68}Ga-SSTR PET to the most ^{18}F-FDG–avid tumor lesion, the median OS was higher than in patients with a ratio of less than 2 ($P = 0.030$).

One of the limitations of this study is that it was a retrospective analysis (however, with prospective data sampling using a structured database). There were variations in radioisotopes and SSTR affinities because different radiopharmaceuticals were used. Another limitation was the lack of availability of the exact Ki-67 index in 104 (21%) patients; however, these patients were referred from other centers with histopathologically confirmed NENs without reporting the Ki-67 index, and relevant tissue specimens were not available for reevaluation. Furthermore, concerning the value of SSTR uptake for predicting survival after receiving PRRT, this study analyzed only the single highest SUV_{max} among all target lesions on ^{68}Ga-SSTR PET for each patient. Analysis of the metastatic tumor burden score on ^{68}Ga-SSTR PET, the further genomic signature, and the association between survival and comprehensive individual evaluation of SSTR expression remains warranted.

CONCLUSION

^{18}F-FDG PET/CT demonstrating glycolytic activity, or lack thereof, is an independent prognostic factor in patients with NENs treated with PRRT. ^{18}F-FDG–negative NENs demonstrated better OS and PFS than ^{18}F-FDG–positive NENs, particularly in pancreatic NENs. High uptake on ^{68}Ga-SSTR PET/CT combined with negative ^{18}F-FDG PET/CT findings is associated with a comparatively prolonged PFS and OS.

DISCLOSURE

No potential conflict of interest relevant to this article was reported.

ACKNOWLEDGMENTS

We thank the patients who participated in this study, as well as all research support staff, radiopharmacists, radiochemists, physician colleagues, nursing staff, and nuclear medicine technologists, past and present, at Zentralklinik Bad Berka, for their support.

KEY POINTS

QUESTION: Is ^{18}F-FDG PET an independent prognostic factor in patients with NENs treated with PRRT and useful in NEN patients after PRRT?

PERTINENT FINDINGS: This large cohort study revealed the presence of positive lesions on ^{18}F-FDG PET to be an independent prognostic factor in patients with NENs treated with PRRT. A significant difference was found in both PFS and OS between ^{18}F-FDG–positive and ^{18}F-FDG–negative patients.

IMPLICATIONS FOR PATIENT CARE: Metabolic imaging with ^{18}F-FDG PET/CT complements the molecular imaging aspect of ^{68}Ga-SSTR PET/CT for the prognosis of survival in NEN patients after PRRT.

REFERENCES

1. Huguet I, Grossman AB, O'Toole D. Changes in the epidemiology of neuroendocrine tumours. *Neuroendocrinology.* 2017;104:105–111.
2. Modlin IM, Oberg K, Chung DC, et al. Gastroenteropancreatic neuroendocrine tumours. *Lancet Oncol.* 2008;9:61–72.
3. Falconi M, Eriksson B, Kaltsas G, et al. ENETS consensus guidelines update for the management of patients with functional pancreatic neuroendocrine tumors and non-functional pancreatic neuroendocrine tumors. *Neuroendocrinology.* 2016; 103:153–171.
4. Fazio N. Watch and wait policy in advanced neuroendocrine tumors: what does it mean? *World J Clin Oncol.* 2017;8:96–99.
5. Bodei L, Herrmann K, Baum RP, Kidd M, Malczewska A, Modlin IM. Caveat emptor: let our acclaim of the apotheosis of PRRT not blind us to the error of Prometheus. *J Nucl Med.* 2019;60:7–8.
6. Werner RA, Weich A, Kircher M, et al. The theranostic promise for neuroendocrine tumors in the late 2010s: where do we stand, where do we go? *Theranostics.* 2018;8:6088–6100.
7. Strosberg J, El-Haddad G, Wolin E, et al. Phase 3 trial of ^{177}Lu-dotatate for midgut neuroendocrine tumors. *N Engl J Med.* 2017;376:125–135.
8. Baum RP, Kulkarni HR, Carreras C. Peptides and receptors in image-guided therapy: theranostics for neuroendocrine neoplasms. *Semin Nucl Med.* 2012;42: 190–207.
9. Strosberg J, Wolin E, Chasen B, et al. Health-related quality of life in patients with progressive midgut neuroendocrine tumors treated with ^{177}Lu-dotatate in the phase III NETTER-1 trial. *J Clin Oncol.* 2018;36:2578–2584.
10. Baum RP, Kulkarni HR, Singh A, et al. Results and adverse events of personalized peptide receptor radionuclide therapy with ^{90}yttrium and ^{177}lutetium in 1048 patients with neuroendocrine neoplasms. *Oncotarget.* 2018;9:16932–16950.
11. Bodei L, Kidd M, Modlin IM, et al. Measurement of circulating transcripts and gene cluster analysis predicts and defines therapeutic efficacy of peptide receptor radionuclide therapy (PRRT) in neuroendocrine tumors. *Eur J Nucl Med Mol Imaging.* 2016;43:839–851.
12. Kong G, Thompson M, Collins M, et al. Assessment of predictors of response and long-term survival of patients with neuroendocrine tumour treated with peptide receptor chemoradionuclide therapy (PRCRT). *Eur J Nucl Med Mol Imaging.* 2014;41:1831–1844.
13. Panzuto F, Nasoni S, Falconi M, et al. Prognostic factors and survival in endocrine tumor patients: comparison between gastrointestinal and pancreatic localization. *Endocr Relat Cancer.* 2005;12:1083–1092.
14. Bertani E, Fazio N, Radice D, et al. Resection of the primary tumor followed by peptide receptor radionuclide therapy as upfront strategy for the treatment of G1-G2 pancreatic neuroendocrine tumors with unresectable liver metastases. *Ann Surg Oncol.* 2016;23:981–989.
15. Lee ST, Kulkarni HR, Singh A, Baum RP. Theranostics of neuroendocrine tumors. *Visc Med.* 2017;33:358–366.
16. Zhang J, Kulkarni HR, Singh A, Niepsch K, Muller D, Baum RP. Peptide receptor radionuclide therapy in grade 3 neuroendocrine neoplasms: safety and survival analysis in 69 patients. *J Nucl Med.* 2019;60:377–385.
17. Carlsen EA, Fazio N, Granberg D, et al. Peptide receptor radionuclide therapy in gastroenteropancreatic NEN G3: a multicenter cohort study. *Endocr Relat Cancer.* 2019;26:227–239.
18. Aalbersberg EA, Huizing DM, Walraven I, et al. Parameters to predict progression-free and overall survival after peptide receptor radionuclide therapy: a multivariate analysis in 782 patients. *J Nucl Med.* 2019;60:1259–1265.
19. Nicolini S, Severi S, Ianniello A, et al. Investigation of receptor radionuclide therapy with ^{177}Lu-DOTATATE in patients with GEP-NEN and a high Ki-67 proliferation index. *Eur J Nucl Med Mol Imaging.* 2018;45:923–930.
20. Thang SP, Lung MS, Kong G, et al. Peptide receptor radionuclide therapy (PRRT) in European Neuroendocrine Tumour Society (ENETS) grade 3 (G3) neuroendocrine neoplasia (NEN): a single-institution retrospective analysis. *Eur J Nucl Med Mol Imaging.* 2018;45:262–277.
21. Seregni E, Ferrari L, Bajetta E, Martinetti A, Bombardieri E. Clinical significance of blood chromogranin A measurement in neuroendocrine tumours. *Ann Oncol.* 2001;12(suppl 2):S69–S72.
22. Panagiotidis E, Alshammari A, Michopoulou S, et al. Comparison of the impact of ^{68}Ga-DOTATATE and ^{18}F-FDG PET/CT on clinical management in patients with neuroendocrine tumors. *J Nucl Med.* 2017;58:91–96.
23. Haug AR, Auernhammer CJ, Wangler B, et al. ^{68}Ga-DOTATATE PET/CT for the early prediction of response to somatostatin receptor-mediated radionuclide therapy in patients with well-differentiated neuroendocrine tumors. *J Nucl Med.* 2010;51:1349–1356.
24. Rindi G, Kloppel G, Couvelard A, et al. TNM staging of midgut and hindgut (neuro) endocrine tumors: a consensus proposal including a grading system. *Virchows Arch.* 2007;451:757–762.
25. Hellman P, Lundstrom T, Ohrvall U, et al. Effect of surgery on the outcome of midgut carcinoid disease with lymph node and liver metastases. *World J Surg.* 2002;26:991–997.
26. Naraev BG, Ramirez RA, Kendi AT, Halfdanarson TR. Peptide receptor radionuclide therapy for patients with advanced lung carcinoids. *Clin Lung Cancer.* 2019;20:e376–e392.
27. Binderup T, Knigge U, Loft A, Federspiel B, Kjaer A. ^{18}F-fluorodeoxyglucose positron emission tomography predicts survival of patients with neuroendocrine tumors. *Clin Cancer Res.* 2010;16:978–985.
28. Kwee TC, Basu S, Saboury B, Ambrosini V, Torigian DA, Alavi A. A new dimension of FDG-PET interpretation: assessment of tumor biology. *Eur J Nucl Med Mol Imaging.* 2011;38:1158–1170.
29. Van den Wyngaert T, Helsen N, Carp L, et al. Fluorodeoxyglucose-positron emission tomography/computed tomography after concurrent chemoradiotherapy in locally advanced head-and-neck squamous cell cancer: the ECLYPS study. *J Clin Oncol.* 2017;35:3458–3464.
30. Meignan M, Cottereau AS, Versari A, et al. Baseline metabolic tumor volume predicts outcome in high-tumor-burden follicular lymphoma: a pooled analysis of three multicenter studies. *J Clin Oncol.* 2016;34:3618–3626.
31. Hutchings M, Kostakoglu L, Zaucha JM, et al. In vivo treatment sensitivity testing with positron emission tomography/computed tomography after one cycle of chemotherapy for Hodgkin lymphoma. *J Clin Oncol.* 2014;32:2705–2711.
32. Bodei L, Mueller-Brand J, Baum RP, et al. The joint IAEA, EANM, and SNMMI practical guidance on peptide receptor radionuclide therapy (PRRNT) in neuroendocrine tumours. *Eur J Nucl Med Mol Imaging.* 2013;40:800–816.
33. Wehrmann C, Senftleben S, Zachert C, Muller D, Baum RP. Results of individual patient dosimetry in peptide receptor radionuclide therapy with ^{177}Lu DOTA-TATE and ^{177}Lu DOTA-NOC. *Cancer Biother Radiopharm.* 2007;22: 406–416.
34. Baum RP, Kulkarni HR. THERANOSTICS: from molecular imaging using Ga-68 labeled tracers and PET/CT to personalized radionuclide therapy—the Bad Berka experience. *Theranostics.* 2012;2:437–447.
35. Eisenhauer EA, Therasse P, Bogaerts J, et al. New response evaluation criteria in solid tumours: revised RECIST guideline (version 1.1). *Eur J Cancer.* 2009;45: 228–247.
36. Young H, Baum R, Cremerius U, et al. Measurement of clinical and subclinical tumour response using [^{18}F]-fluorodeoxyglucose and positron emission tomography: review and 1999 EORTC recommendations. European Organization for Research and Treatment of Cancer (EORTC) PET study group. *Eur J Cancer.* 1999;35:1773–1782.

37. Khan S, Krenning EP, van Essen M, Kam BL, Teunissen JJ, Kwekkeboom DJ. Quality of life in 265 patients with gastroenteropancreatic or bronchial neuroendocrine tumors treated with [^{177}Lu-DOTA0,Tyr3]octreotate. *J Nucl Med.* 2011;52:1361–1368.
38. Deppen SA, Liu E, Blume JD, et al. Safety and efficacy of ^{68}Ga-DOTATATE PET/CT for diagnosis, staging, and treatment management of neuroendocrine tumors. *J Nucl Med.* 2016;57:708–714.
39. Gabriel M, Decristoforo C, Kendler D, et al. ^{68}Ga-DOTA-Tyr3-octreotide PET in neuroendocrine tumors: comparison with somatostatin receptor scintigraphy and CT. *J Nucl Med.* 2007;48:508–518.
40. Nilica B, Waitz D, Stevanovic V, et al. Direct comparison of ^{68}Ga-DOTA-TOC and ^{18}F-FDG PET/CT in the follow-up of patients with neuroendocrine tumour treated with the first full peptide receptor radionuclide therapy cycle. *Eur J Nucl Med Mol Imaging.* 2016;43:1585–1592.
41. Sansovini M, Severi S, Ianniello A, et al. Long-term follow-up and role of FDG PET in advanced pancreatic neuroendocrine patients treated with ^{177}Lu-DOTATATE. *Eur J Nucl Med Mol Imaging.* 2017;44:490–499.
42. Paganelli G, Sansovini M, Scarpi E. Reply to: predicting the outcome of peptide receptor radionuclide therapy in neuroendocrine tumors: the importance of dual-tracer imaging. *Eur J Nucl Med Mol Imaging.* 2017;44:1777–1778.
43. Chan DL, Pavlakis N, Schembri GP, et al. Dual somatostatin receptor/FDG PET/CT imaging in metastatic neuroendocrine tumours: proposal for a novel grading scheme with prognostic significance. *Theranostics.* 2017;7:1149–1158.
44. Miederer M, Seidl S, Buck A, et al. Correlation of immunohistopathological expression of somatostatin receptor 2 with standardised uptake values in ^{68}Ga-DOTATOC PET/CT. *Eur J Nucl Med Mol Imaging.* 2009;36:48–52.